Atmospheric
Measurement
Techniques

Supplement of

Measurement of carbonaceous aerosol with different sampling configurations and frequencies

Y. Cheng and K.-B. He

Correspondence to: K.-B. He (ycheng@mail.tsinghua.edu.cn, hekb@tsinghua.edu.cn)

Section-1: Evaluation of the activated carbon denuder.

Four factors were considered when evaluating the activated carbon denuder:

(1) Denuder breakthrough and efficiency. Denuder breakthrough, defined as the amount of gaseous organics that are not removed by the denuder and subsequently adsorbed by the filter downstream, was measured by the "breakthrough channel". The "breakthrough channel" was the same as channel 1 (see Table 1 in the main manuscript), expect that a quartz filter (i.e., the TSP filter; TSP refers to total suspended particulate matter) was placed upstream of the $PM_{2.5}$ cyclone. In the "breakthrough channel", particles were removed by the TSP filter, and gaseous organics were captured by the charcoal denuder. As a result, OC measured on the quartz filters downstream of the denuder was from breakthrough. In this study, breakthrough OC averaged 0.27 ± 0.13 $\mu gC/cm^2$, comparable with filter blank OC (averaging 0.43 ± 0.12 $\mu gC/cm^2$). Therefore, the activated carbon denuder used in this study is able to effectively remove the gaseous organics that could be adsorbed by quartz filters (i.e., is able to remove the positive sampling artifact with an efficiency of 100%).

(2) Particle loss due to the diffusion to the walls of the denuder. Particle loss can be evaluated by comparing EC concentrations measured by channel 1 (denuded) and 2 (un-denuded) (see Table 1 in the main manuscript). EC concentrations (24 h averaged values) measured by these two channels correlated well with a slope of 0.98 ± 0.01 ($R^2 = 0.91$), while results from the paired-t test suggested that they were not significantly different at a 95% level of confidence (2-tailed $p = 0.126$). Therefore, the particle loss in the denuder was negligible in this study.

(3) Evaporation of particulate OC during passage through the denuder. This effect should be negligible if the residence time of particles in the denuder is less than 0.2 s. In this study, the residence time was 0.18 s, indicating that the evaporation of particulate OC in the denuder was

minimal.

(4) Shedding of the denuder material (activated carbon). No tiny charcoal particles were observed on the denuded filters throughout the measurement period. Moreover, results from the OC/EC analysis showed that no EC was detected on the front quartz filter in the breakthrough channel, demonstrating the contamination due to the shedding of the denuder material was negligible.

Section-2: Problems in the comparison of ATN measured by the carbon analyzer and the filter-based, online instruments.

Although the measurement of ATN by the carbon analyzer is similar to that based on the filter-based, online instruments such as the Aethalometer and the PSAP, ATN retrieved from these two types of techniques should be compared with caution. In the carbon analyzer, the transmittance signal is monitored at only one wavelength, which is 632 and 678 nm for the DRI and Sunset analyzers, respectively. In the online instruments such as the Aethalometer and the PSAP, the transmittance signal is usually measured at several different wavelengths (a commonly used one is 550 nm). Therefore, when comparing ATN retrieved from these two types of techniques, the difference in the measurement wavelength needs to be accounted for, which can be done if the absorption Ångström exponent is known. Moreover, the primary purpose of the carbon analyzer is to determine OC and EC. Thus, compared to the Aethalometer and the PSAP, filter loading might be much higher when operating the carbon analyzer, indicating that ATN retrieved from the carbon analyzer might be more strongly biased by the artifacts associated with filter loading (e.g., the shadowing effect).

Section-3: Statistical results for the comparisons, regressions and ratios included in this paper.

Table S-1. Statistical results for the ratios and regressions included in this study.

Y	X	Y/X	Slope	R^2
Performance of the carbon analyzer				
TC parallel-1	TC parallel-2	1.00 ± 0.02	0.99 ± 0.00	0.99
ATN parallel-1	ATN parallel-2	1.01 ± 0.07	1.01 ± 0.02	0.94
OC_T parallel-1	OC_T parallel-2	1.00 ± 0.02	0.99 ± 0.00	0.99
EC_T parallel-1	EC_T parallel-2	1.01 ± 0.05	1.00 ± 0.01	0.93
OC_R parallel-1	OC_R parallel-2	0.99 ± 0.03	0.98 ± 0.01	0.99
EC_R parallel-1	EC_R parallel-2	1.01 ± 0.03	1.02 ± 0.01	0.99
Comparison of 48 h averaged TC, OC, EC measured by different sampling configurations and frequencies during the low RH period				
Low-frequency TC_{BQ}	High-frequency TC_{DQ}	1.18 ± 0.08	1.16 ± 0.02	0.98
Low-frequency TC_{BQ-QBQ}	High-frequency TC_{DQ}	1.04 ± 0.07	1.03 ± 0.02	0.98
High-frequency TC_{BQ}	High-frequency TC_{DQ}	1.33 ± 0.09	1.30 ± 0.02	0.98
High-frequency TC_{BQ-QBQ}	High-frequency TC_{DQ}	1.16 ± 0.10	1.13 ± 0.02	0.97
Low-frequency OC_{BQ}	High-frequency OC_{DQ}	1.31 ± 0.13	1.25 ± 0.04	0.95
Low-frequency OC_{BQ-QBQ}	High-frequency OC_{DQ}	1.12 ± 0.11	1.08 ± 0.02	0.98
High-frequency OC_{BQ}	High-frequency OC_{DQ}	1.48 ± 0.17	1.40 ± 0.04	0.96
High-frequency OC_{BQ-QBQ}	High-frequency OC_{DQ}	1.23 ± 0.16	1.17 ± 0.03	0.96
Low-frequency EC_{BQ}	High-frequency EC_{DQ}	0.86 ± 0.11	0.87 ± 0.05	0.73
High-frequency EC_{BQ}	High-frequency EC_{DQ}	0.99 ± 0.04	0.99 ± 0.02	0.95
Comparison of 48 h averaged TC, OC, EC measured by different sampling configurations and frequencies during the high RH period				
Low-frequency TC_{BQ}	High-frequency TC_{DQ}	0.95 ± 0.05	0.95 ± 0.02	0.90
Low-frequency TC_{BQ-QBQ}	High-frequency TC_{DQ}	0.84 ± 0.05	0.84 ± 0.02	0.90
High-frequency TC_{BQ}	High-frequency TC_{DQ}	1.16 ± 0.04	1.15 ± 0.01	0.96
High-frequency TC_{BQ-QBQ}	High-frequency TC_{DQ}	1.04 ± 0.03	1.04 ± 0.01	0.97
Low-frequency OC_{BQ}	High-frequency OC_{DQ}	0.99 ± 0.09	0.98 ± 0.03	0.78
Low-frequency OC_{BQ-QBQ}	High-frequency OC_{DQ}	0.85 ± 0.08	0.84 ± 0.03	0.74
High-frequency OC_{BQ}	High-frequency OC_{DQ}	1.21 ± 0.06	1.21 ± 0.02	0.92
High-frequency OC_{BQ-QBQ}	High-frequency OC_{DQ}	1.07 ± 0.05	1.07 ± 0.02	0.93
Low-frequency EC_{BQ}	High-frequency EC_{DQ}	0.83 ± 0.09	0.83 ± 0.03	0.67
High-frequency EC_{BQ}	High-frequency EC_{DQ}	0.96 ± 0.06	0.96 ± 0.02	0.81

Table S-1 (continued). Statistical results for the ratios and regressions included in this study.

Y	X	Y/X	Slope	R^2
Comparison of 48 h integrated ATN measured by different sampling configurations and frequencies				
Low-frequency ATN_{BQ}	Integrated high-frequency ATN_{DQ}	0.89 ± 0.05	0.89 ± 0.02	0.93

Tables S-2. The 2-tailed *p* values for the major comparisons included in this study (2-tailed p < 0.1 indicates significant difference at a 95% level of confidence, whereas 2-tailed *p* > 0.1 indicates insignificant difference).

Y	X	2-tailed p	Note
RH in the high RH period	RH in the low RH period	**0.000**	Independent t-test; 24 h averages
Low-frequency TC_{BQ} during the high RH period	High-frequency TC_{DQ} during the high RH period	**0.044**	Paired t-test; 48 h averages
Low-frequency EC_{BQ}	High-frequency EC_{DQ}	**0.000**	Paired t-test; 48 h averages
High-frequency EC_{BQ}	High-frequency EC_{DQ}	0.113	Paired t-test; 48 h averages
Low-frequency ATN_{BQ}	Integrated high-frequency ATN_{DQ}	**0.000**	Paired t-test; 48 h integrated values
EC_R to EC_T ratios of the low frequency samples	EC_R to EC_T ratios of the high frequency, denuded samples	**0.005**	Independent t-test

Section-4: Comparison of the RH data obtained from Weather Underground and from the China Meteorological Data Sharing Service System.

In addition to those from Weather Underground, RH data for Beijing were also available from the China Meteorological Data Sharing Service System (http://cdc.cma.gov.cn/home.do), including daily averaged values measured at three sites: one sub-urban site (site 1; 39.8° N, 116.47° E) and two rural sites (site 2 and 3, located at 40.38° N, 116.87° E and 40.45° N, 115.97° E, respectively). As shown in Figure S-1, RH obtained from these two sources exhibited quite similar daily variations, and particularly, agreed well with respect to the identification of the high RH period.
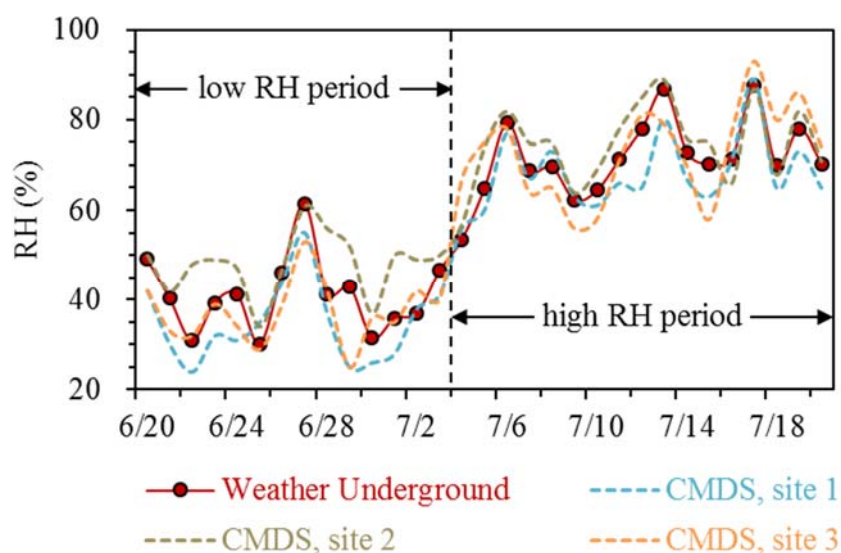

Figure S-1. Daily variations of RH (24 h averages calculated between 00:00 and 23:59) in Beijing during the measurement period of this study. Results from Weather Underground and CMDS (the China Meteorological Data Sharing Service System) are shown separately.

Section-5: Comparison of TC, OC and EC measured by different sampling configurations and frequencies: scatter plots.
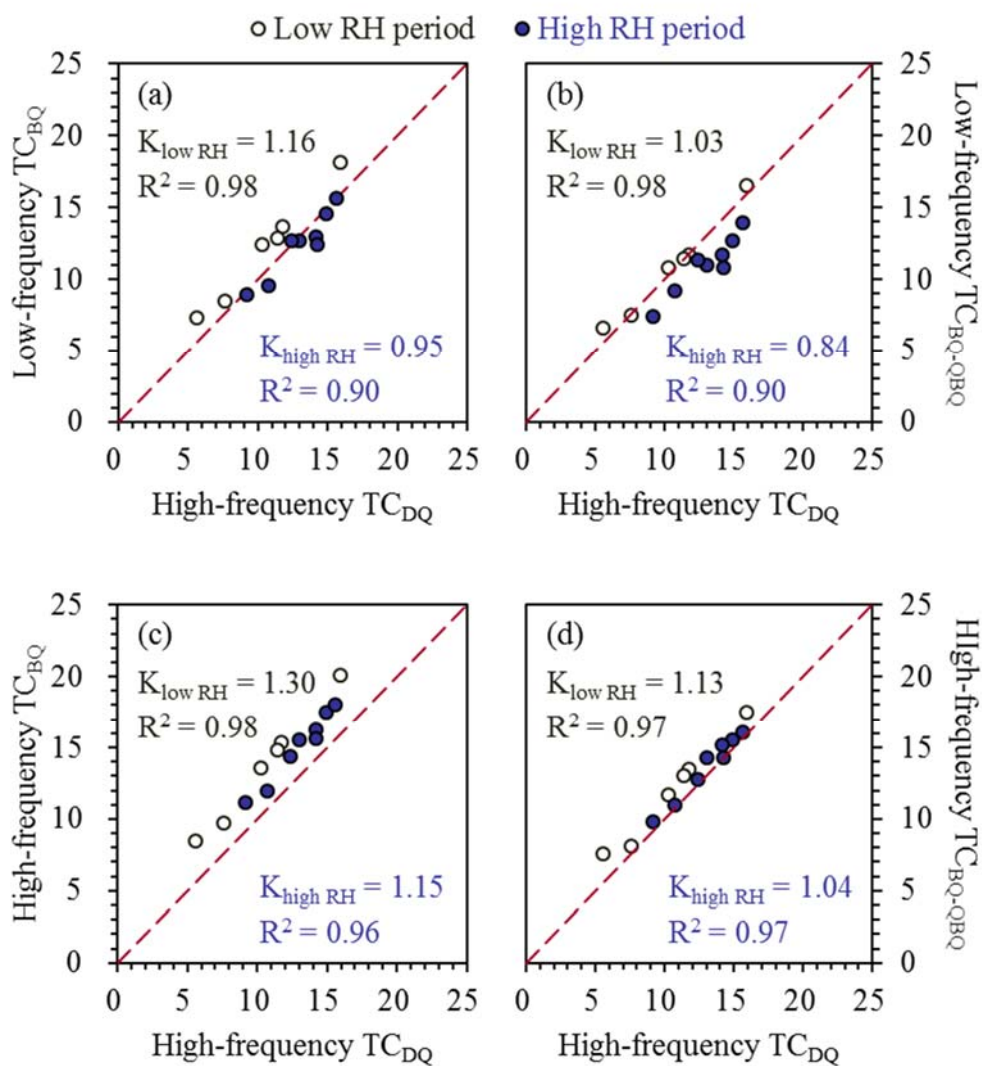

Figure S-2. Comparison of TC concentrations ($\mu gC/m^3$) measured by different sampling configurations and frequencies. Linear regression results are shown with K as slope (intercept is set as zero). The dashed lines indicate one-to-one correspondence.
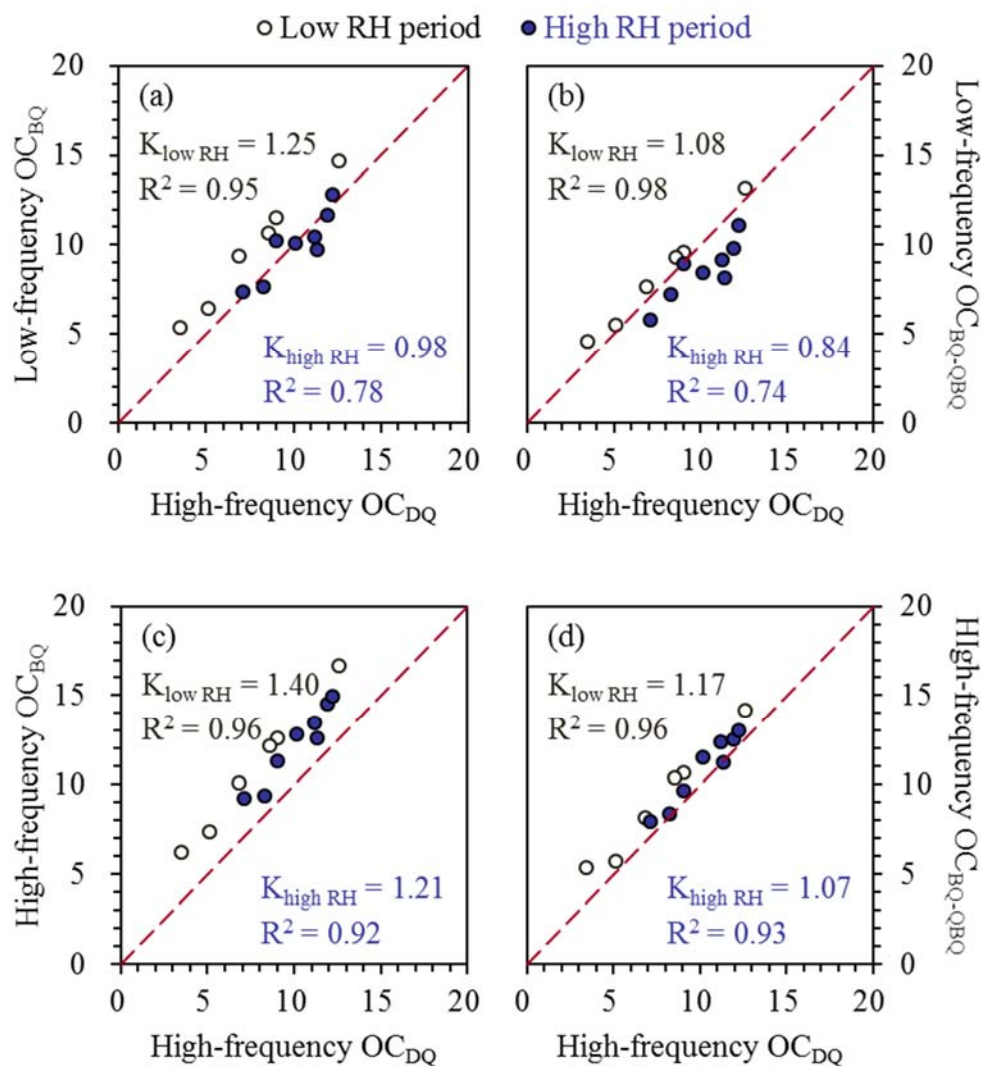
Figure S-3. Comparison of OC concentrations ($\mu gC/m^3$) measured by different sampling configurations and frequencies. Linear regression results are shown with K as slope (intercept is set as zero). The dashed lines indicate one-to-one correspondence.
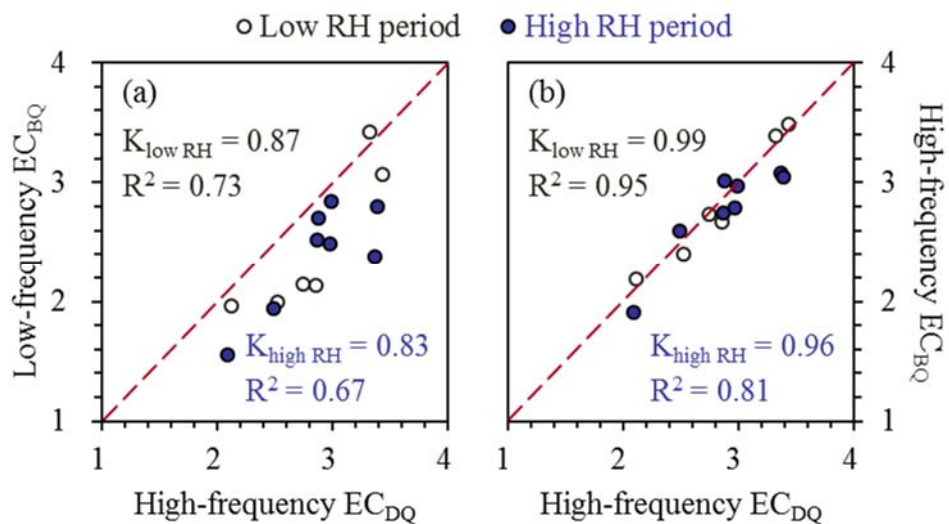
.

Figure S-4. Comparison of EC concentrations ($\mu gC/m^3$) measured by different sampling configurations and frequencies. Linear regression results are shown with K as slope (intercept is set as zero). The dashed lines indicate one-to-one correspondence.